Photocatalytic Oxidation of 2-Chloroethyl Ethyl Sulfide on TiO_2-SiO_2 Powders

D. A. Panayotov, D. K. Paul, and J. T. Yates, Jr.*

Department of Chemistry, Surface Science Center, University of Pittsburgh, Pittsburgh, Pennsylvania 15260

Received: April 22, 2003; In Final Form: July 14, 2003

The photocatalytic oxidation of 2-chloroethyl ethyl sulfide (2-CEES, a simulant for mustard gas) on high area TiO_2-SiO_2 powder has been studied by transmission infrared spectroscopy. It has been found that the photocatalytic oxidation of 2-CEES occurs on the surface of TiO_2-SiO_2 at 200 K with an appreciable rate, causing 40−50% depletion of the initial surface coverage before the photoreaction slows down appreciably. In addition to 2-CEES, we have also studied the photooxidation of diethyl sulfide (DES), as a comparison, to test the role of Cl substitution in the 2-CEES molecule. With both 2-CEES and DES, partially and fully oxidized products are observed. By comparison of the spectral developments during the photooxidation of 2-CEES and DES, it appears that the presence of the chlorine substituent in 2-CEES is not strongly influential in the photooxidation sequences for this molecule. The 2-CEES molecule is hydrogen-bonded to the Si−OH groups by both the Cl and the S moieties, and photooxidation leads to loss of the spectral features caused by hydrogen bonding as the 2-CEES molecule is destroyed.

I. Introduction

Titania−silica (TiO_2-SiO_2)-based mixed oxides have aroused considerable interest as attractive materials for catalytic applications because of their high catalytic activity and selectivity.[1,2] Silica-supported titanium oxide has been reported to exhibit a different photocatalytic performance from that of titania itself.[3] This is partially explained in terms of the interaction between titanium oxide and silica, and also of the different structure of surface titanate from that of bulk titania.[2,4,5] In their review, Wachs and co-workers[2] discussed the relation between the surface titanium oxide structure, the preparation method, and the composition of binary TiO_2-SiO_2 oxides. The authors concluded that the intimate interaction of TiO_2 and SiO_2 may result in new structural characteristics and physicochemical/reactivity properties. Mixed TiO_2-SiO_2 oxides, prepared by the sol−gel process has been shown to exhibit different surface chemical and photochemical properties as the result of the mixed coordination to lattice O via Ti−O−Si linkages. However, these linkages may decompose upon sintering of the material, causing phase segregation into TiO_2 and SiO_2 phases,[2,6] and we believe that this is the case in the samples studied here.

The 2-chloroethyl ethyl sulfide (2-CEES) molecule is a simulant for mustard gas. The DES molecule is used in this work as a comparison molecule to 2-CEES to test the role of Cl substitution in the 2-CEES. Mustard gas contains two chloroethyl groups instead of the single chloroethyl group of 2-CEES. A highly promising universal method for the destruction of various airborne and dissolved organics is photocatalytic oxidation on TiO_2.[7,8] The photocatalytic oxidation of thioethers,[9] DES,[10] and 2-CEES[11] has been found to proceed over TiO_2 powder under ambient conditions. Different routes have been discussed[9−11] in order to understand the mechanism of the photooxidation reaction.

Studying the photocatalytic oxidation of thioethers on irradiated TiO_2 powders, Fox and Abdel-Wahab[9] have established that the C−S bond cleavage dominates the photocatalytic degradation of dibenzyl sulfide, whereas sulfoxide formation ensues from diaryl sulfides.

On the basis of the set of detected products, Vorontsov et al.[10] have proposed the following four general routes for the initial transformation of diethyl sulfide: (1) hydrolysis of DES via C−S bond cleavage, giving ethanol and ethylene as primary products; (2) oxidation of the sulfur atom to sulfoxide and sulfone; (3) oxidation at the α-carbon to produce $CH_3CH_2-S-CO-CH_3$ which then transforms to ethyl acetate; (4) oxidation at the β-carbon to form $CH_3CH_2SCH_2CH_2OH$. The "C−S cleavage" branch is considered to be the main route of diethyl sulfide photooxidation over TiO_2. During the further deeper reaction to more highly oxidized products, these routes can intersect each other. Finally, the photocatalytic oxidation results in production of inorganic oxides, H_2O, CO_2, and SO_2.

Since disulfides, rather than sulfoxide and sulfone, were detected as products during the photooxidation of 2-CEES over TiO_2 powder (Degussa P25), Martyanov and Klabunde[11] have suggested the formation of the surface hydroxyl radical as the primary oxidizing species. The proposed mechanism includes formation of the thioether α-carbon radical. The α-carbonyl radical may thermally decompose to ethylene and surface thiyl radical; or after stabilization with oxygen, attack by water may yield the thiyl radical and ethanol. Further oxidation of ethanol can give acetaldehyde. Both the alkyl and Cl moieties of 2-CEES are involved in the reaction. Acetaldehyde, ethylene, chloroacetaldehyde, chloroethylene, and disulfides are found as primary oxidation products. Formation of disulfides has a blocking effect. Elevated water content accelerates the disulfides' disappearance, and simultaneously facilitates more rapid, deep oxidation of 2-CEES.

Therefore the C−S bond cleavage and the oxidation at the α-carbon position can be considered as the main routes for 2-CEES photocatalytic oxidation.

It was recently established that during adsorption on both TiO_2 and a TiO_2-SiO_2 composite, hydrogen bonding of the 2-CEES molecule to surface Si−OH groups occurs through both the Cl and the S moieties.[12] It was found that the Cl atom in

* Corresponding author. E-mail: jyates@pitt.edu.

10.1021/jp030489t CCC: $25.00
Published on Web 08/28/2003

2-CEES forms a spectroscopically characteristic hydrogen bond with Si−OH groups. In addition, the S atom also forms a characteristic hydrogen bond to Si−OH.

In our experiment, the temperature of the 2-CEES and DES adsorption systems is maintained at 200 K by means of electrical control. This prevents thermally activated chemical reactions from occurring in combination with the primary photooxidation reactions, and allows direct observation of the photochemical processes. At 200 K, we know that diffusion of the adsorbed 2-CEES and DES molecules occurs throughout the depth of the powdered photocatalyst.[12]

In this paper, we use transmission infrared spectroscopy to characterize the surface species formed during the photooxidation of 2-CEES and DES in order to understand the factors, which may, in turn, influence the photooxidation of mustard gas.

II. Experimental Section

The powdered samples were hydraulically pressed at 12000 lbs/in^2 into a fine-tungsten support grid[13] (0.0508 mm thick, with 0.22 mm^2 square holes) as a circular spot 7 mm in diameter. The grid is held by nickel heating and cooling supports in the center of the dual beam IR−UV photoreactor. The grid is mounted in the cell at a 45° angle to the IR beam, so that irradiation of the grid with ultraviolet light directed perpendicularly to the IR beam can be carried out without making a geometrical change. Electrical heating and cooling with liquid nitrogen permit the temperature of the grid to be set within the range 100−1500 K. A type K thermocouple, spot welded to the top of the grid, is used for temperature control. Steady-state temperatures are maintained electrically to ±2K, using an electronic programmer[14] that senses the output of the thermocouple. The grid is 80% transparent, so that infrared radiation can pass through the sample efficiently. The cell gas outlet is connected to an ultrahigh vacuum system, equipped with a mass spectrometer. Both a Pfeiffer Vacuum 60 L/s turbomolecular pump and a Varian 20 L/s ion pump are used to maintain the base pressure of the system below 10^{-7} Torr. A Baratron capacitance manometer is utilized for measuring the gas pressures. The cell windows were KBr single crystals mounted on concentric Viton O-rings which are differentially pumped to prevent leaks. A more detailed description of the cell may be found in refs 15−17.

The dual beam IR−UV photoreactor is mounted on a translation system (Newport Corporation). The translation system is computer-controlled and capable of moving the cell to ±1 μm accuracy in the horizontal and vertical directions.[16] This allows one to record spectra for two samples and for the background (an empty position on the grid) in the same experiment. Thus, it is possible to employ two samples at different positions on the same grid for comparison of their catalytic behavior under identical conditions of temperature and gas exposure.

The ultraviolet light source was a 350 W high-pressure Hg arc (Oriel Corp.[18]) which was focused onto the sample through a KBr window. The light was filtered with a water filter to remove IR radiation. The intensity of the UV radiation on the sample was 240 mW/cm^2 in the energy range 2.1−5 eV.

The infrared spectrometer was a Mattson Research Series I FTIR, and all scans were made in the ratio mode with a resolution of 4 cm^{-1}. Typically, 200 scans were accumulated in each spectrum.

The TiO_2−SiO_2 sample was prepared in the laboratory of Professor K. Klabunde, Kansas State University, by a sol−gel technique. The texture characteristic of the TiO_2/SiO_2 were as follows: surface area 680 m^2/g; pore volume 2.97 cm^3/g; and average pore diameter 175 Å. The composition of the TiO_2−SiO_2 sample was 50 mol % TiO_2 and 50 mol % SiO_2. It was heated in vacuum at 673 K for 4 h and then treated with 6.2 Torr O_2 for 0.5 h at the same temperature. It was then heated in a vacuum to 1026 K for 3 h, causing Ti−OH groups to be removed and leaving only Si−OH groups behind.[12]

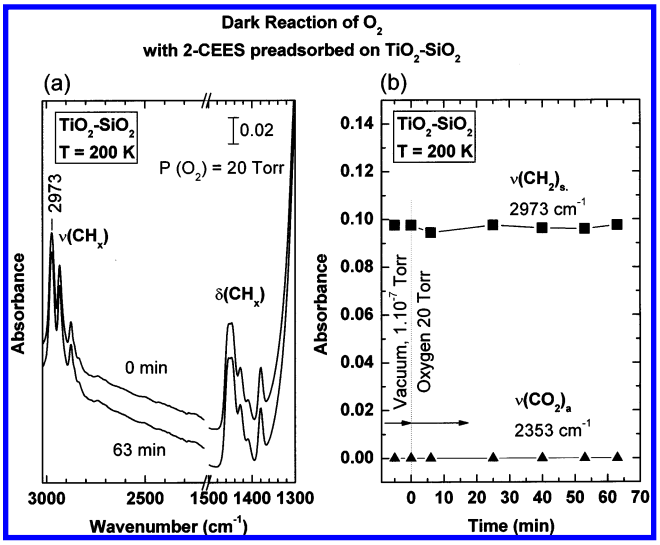

Figure 1. Control experiment showing the absence of a dark reaction between 2-CEES and O_2 at 200 K.

2-Chloroethyl ethyl sulfide (98%) and diethyl sulfide (98%) used for this work was obtained from Aldrich. These liquids were transferred under nitrogen gas to glass bulbs and purified by five freeze−pump−thaw cycles. The vapor was transferred to the infrared cell from the glass bulbs attached to the stainless steel gas line. Ethyl chloride (EC), stored in a metal cylinder, was also obtained from Aldrich and was 99.7% pure. The oxygen used is obtained from VWSCO and was 99.8% pure.

III. Experimental Results

A. Suppression of Thermally Activated Reactions at 200 K. Figure 1a shows a portion of the infrared spectrum for a 2-CEES adsorption experiment where the adsorbed molecule is exposed to O_2(gas) at 200 K without irradiation with UV light. It is seen that over a time period of 63 min, no significant changes in the infrared spectrum are observed under 20 Torr oxygen pressure. Selected absorbances for the CH_2 (symmetric stretch) and in the region of the adsorbed CO_2 (asymmetric stretch) mode are plotted in Figure 1b. No loss of absorbance is observed for $\nu(CH_2)_s$, and adsorbed CO_2 is not produced in this control experiment as shown in Figure 1b. These results indicate that the photooxidation experiments to be shown may be considered to be uninfluenced by thermal reactions of the parent molecule at 200 K.

B. Spectral Changes in Si−OH and $\nu(CH_x)$ Regions during Photooxidation of 2-CEES. Figure 2a shows the hydroxyl stretching region for the initial coverage of 2-CEES and the changes in this region as photooxidation occurs. Some of the isolated Si−OH modes at about 3747 cm^{-1} have been hydrogen-bonded to the 2-CEES molecules through the Cl moiety ($\nu_{OH...Cl}$ = 3606 cm^{-1}) or to the S moiety ($\nu_{OH...S}$ = 3361 cm^{-1}) during adsorption, and this bifunctional bonding of 2-CEES has been reported elsewhere.[12] As photooxidation takes place over a period of 240 min, the intensity of the two hydrogen-bonded Si−OH modes decreases as 2-CEES mol-

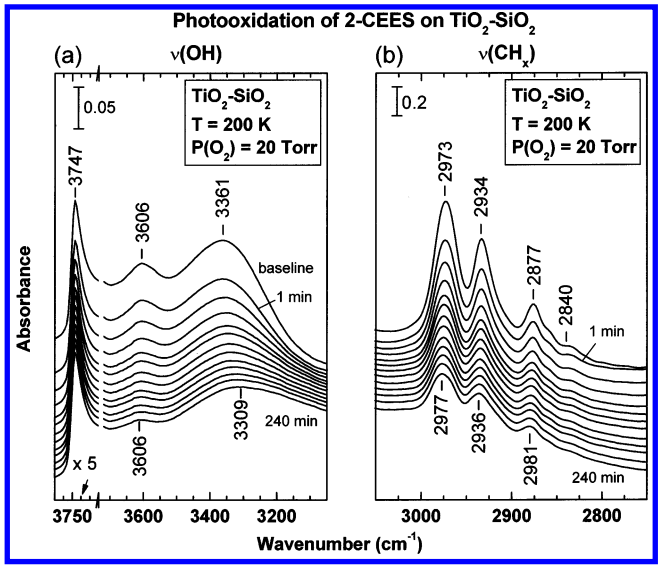

Figure 2. Consumption of 2-CEES hydrogen-bonded to Si−OH groups by photooxidation at 200 K.

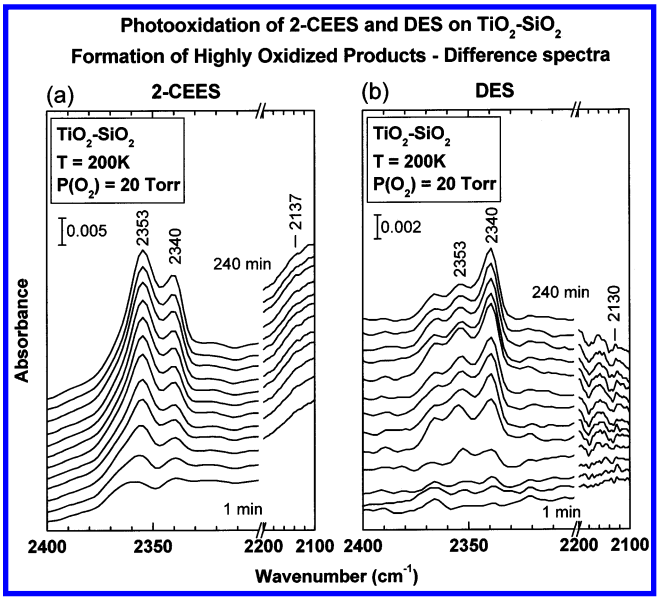

Figure 3. Production of oxidized products from photooxidation of 2-CEES at 200 K.

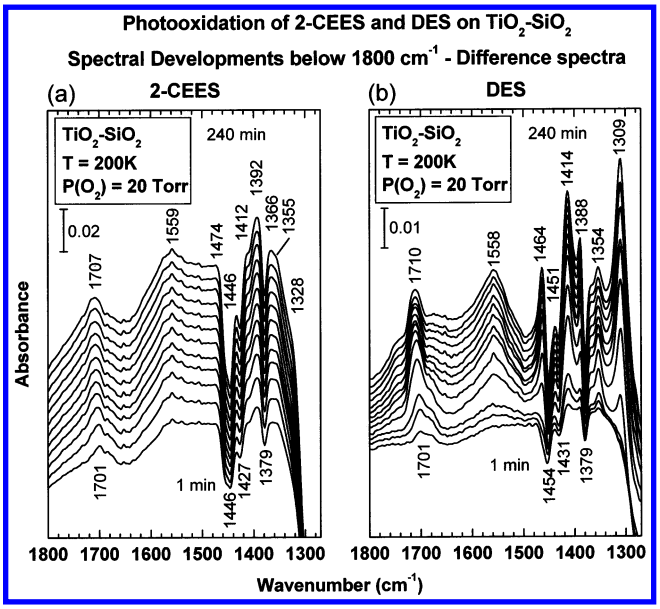

Figure 4. Difference spectra for photooxidation of 2-CEES and DES.

ecules are destroyed. The intensity of the isolated Si−OH mode also decreases slightly, suggesting that the products of the photooxidation of 2-CEES are also hydrogen-bonded so that the isolated Si−OH modes are not regenerated, and indeed a more strongly shifted hydrogen-bonded Si−OH mode at about 3309 cm^{-1} is revealed after extensive photooxidation has been achieved. The observation suggests that oxidized organic species containing carbonyl or sulfonate groups or product water molecules are more strongly hydrogen-bonded to Si−OH groups than the original 2-CEES molecules. Figure 2b shows that the CH_x stretching modes characteristic of the CH_2 and CH_3 groups in 2-CEES are depleted during photooxidation. The fact that new CH_x stretching modes in this spectral region are not clearly observed to be produced during photooxidation indicates that C−H bond oxidation is occurring extensively, and that any intermediate species containing CH_x bonds are of low surface coverage.

C. Spectral Developments for Highly Oxidized Products for 2-CEES and DES Photooxidation. The production of both adsorbed CO and adsorbed CO_2 is observed for both 2-CEES and DES photooxidation at 200 K as shown in Figure 3. Low intensity features near 2130 cm^{-1} for CO(a) and a continuous increase in absorbance at ∼2340−2353 cm^{-1} for CO_2(a) are observed as photooxidation occurs. These are near-final (CO) or final (CO_2) oxidation products, often called mineralization products because of the extreme level of oxidation which they represent. They must represent the result of multiple elementary photooxidation steps as molecules as complex as 2-CEES and DES are destroyed by the production of a sequence of intermediate oxidation products which ultimately reach CO(a) and CO_2(a) products.

D. Spectral Developments below 1800 cm^{-1} for 2-CEES and DES Photooxidation. The spectral region below 1800 cm^{-1} contains a complex overlap of vibrational modes which undergo systematic changes in absorbance as photooxidation of both 2-CEES and DES takes place. The observation of modes which increase and decrease in absorbance can be observed most conveniently by presenting difference spectra obtained over the course of the photooxidation experiments, and this is done in Figure 4. A strongly similar pattern of overlapping bands which either appear or disappear is observed for both 2-CEES and DES. Table 1 summarizes these results and presents a tentative assignment of each mode. Simultaneous growth of bands, attributed to various carbonyl stretching modes due to aldehyde, carboxylate, formate, and carbonate are observed, as shown in Figure 4 and in Table 1.

E. Selected Kinetics Results for 2-CEES Photooxidation Using Infrared Absorbances. Figure 5 gives a summary of the rates of photooxidation as observed from the changes in infrared absorbances as observed for 2-CEES photooxidation at 200 K. In panels (a) and (b), the rate of depletion of absorbances for the CH_2 and CH_3 modes is shown. In panels (c), (d), and (e) the kinetics of production of certain species is shown. These plots allow us to kinetically scale the kinetics of the consumption and development of absorbances for various products of the photooxidation process by providing an approximate "half-life" time constant for depletion of the reactant molecule against which the time constant for production of various products can be compared. A vertical bar symbol, $\tau_{1/2}$, represents the time constant characteristic of each particular absorbance. The baseline against which these peak absorbances are measured is empirically adjusted to compensate for baseline shifts which have been characterized in other investigations.[19]

TABLE 1: Spectral Changes during the Photooxidation of 2-CEES and DES over TiO_2-SiO_2

2-CEES band (cm^{-1})	2-CEES assignment	DES band (cm^{-1})	DES assignment
	Spectral Features of Adsorbed Species Produced in Photooxidation		
2353	CO_2	2353	CO_2
2137	CO	2130	CO
1707	carbonyl $\nu(C{=}O)_{as}$	1710	carbonyl $\nu(C{=}O)_{as}$
1559	carboxyl $\nu(O-C-O)_{as}$	1558	carboxyl $\nu(O-C-O)_{as}$
–		1464	$\nu(CO_2)_{ad}$ (carbonate)
1412	carboxyl $\nu(O-C-O)_s$	1414	carboxyl $\nu(O-C-O)_s$
1392	$\delta(CH)_s$ (formate)	1388	$\delta(CH)_s$ (formate)
1366	carboxyl $\nu(O-C-O)_s$ (formate)	1354	carboxyl $\nu(O-C-O)_s$ (formate)
–		1309	$\nu(CO_2)_{ad}$ (carbonate)
	Spectral Features of Adsorbed Species Depleted in Photooxidation		
1446	$\delta(CH_3)_{as}$, (CH_3-S-)	1451	$\delta(CH_3)_{as}$, (CH_3-S-)
1427	$\delta(CH_2)_{as}$, (CH_2-S-)	1431	$\delta(CH_2)_{as}$, (CH_2-S-)
1379	$\delta(CH_3)_s$, (CH_3-S-)	1379	$\delta(CH_3)_s$, (CH_3-S-)

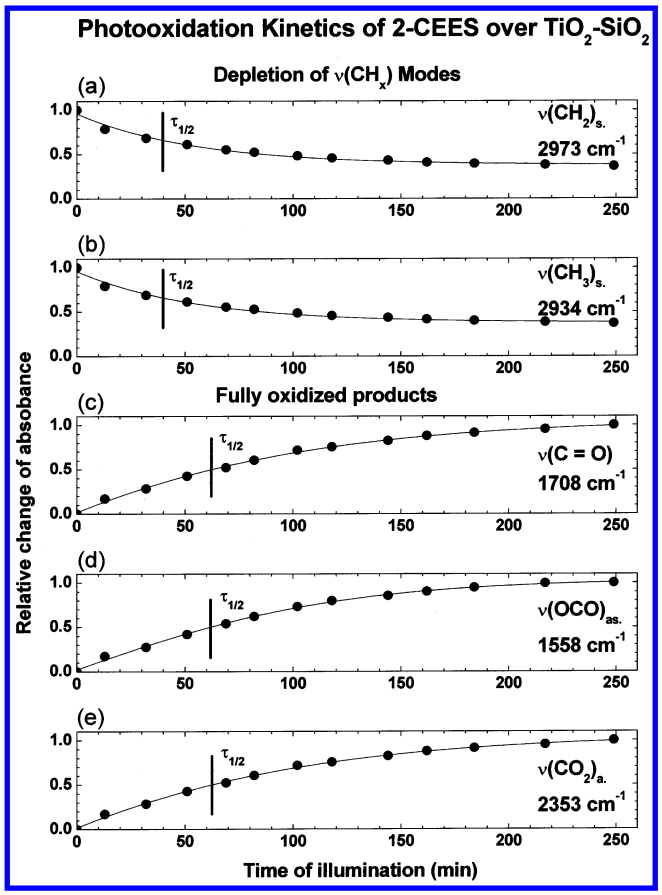

Figure 5. Kinetic behavior for consumption of 2-CEES during photooxidation and for production of highly oxidized products.

These baseline shifts correspond to the production and consumption of trapped conduction band electrons as the photochemistry progresses. A more sophisticated kinetic comparison is not warranted by the data.

F. Kinetic Limit of 2-CEES Photooxidation Chemistry. The kinetic behavior of the CH_3 and CH_2 absorbances indicate that after about 200 min of photooxidation, the 2-CEES depletion rate becomes very small. Two explanations may be offered for this phenomenon: (1) Ultraviolet light is effectively extinguished in the powder at depths which are of the order of 2/3 of the total depth, and diffusion of fresh reactant from the deeper regions to depleted regions of the catalyst does not occur; or (2) Oxidation products build upon the surface of the photocatalyst throughout the depth of the catalyst bed, and prevent O_2 adsorption and activation as the photo reaction proceeds. These two models are now under study in separate experiments.

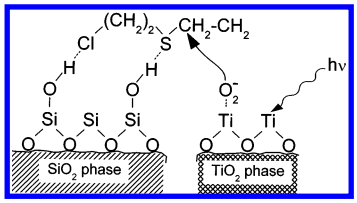

Figure 6. Schematic picture of photooxidation of 2-CEES bound by hydrogen bonding to the SiO_2 phase in a mixed TiO_2-SiO_2 photocatalyst.

IV. Discussion of Results

A. Photochemical Destruction of 2-CEES on TiO_2-SiO_2 Photocatalyst-Site Locations before Reaction. The bonding of the 2-CEES molecule to the surface of the TiO_2-SiO_2 photocatalyst occurs through hydrogen bonding to Si−OH groups which exist as isolated functional groups on the SiO_2 portion of the mixed oxide surface.[12] This bonding occurs by the bifunctional bonding of the 2-CEES molecule through the S and Cl moieties.[12] In contrast, the photoactivation of adsorbed O_2 must certainly occur on the TiO_2 phase of the mixed oxide catalyst, since it is within this phase that band gap excitation of electron−hole pairs is known to occur. Thus, the excited oxygen species which is active in the photooxidation process must be transported over the catalyst from the TiO_2 phase to meet the 2-CEES molecules held on the Si−OH groups some distance away. Our experiments show that these hydrogen-bonded 2-CEES molecules are in fact depleted from the Si−OH groups by photooxidation, as seen in Figure 2a. This process is schematically shown in Figure 6.

B. Destruction of Alkyl Functionalities. Figure 2b shows that the absorbances of the CH_2 and CH_3 vibrational modes of the adsorbed 2-CEES molecule are significantly attenuated during 240 min of photooxidation. Simultaneously, various carbonyl stretching modes due to aldehyde, carboxylate, and formate are developed, as shown in Figure 4 and in Table 1. In addition, both adsorbed CO and adsorbed CO_2 species are produced during photooxidation. In the previous papers, reporting the photocatalytic oxidation of 2-CEES[11] and DES[10] on TiO_2 catalyst, aldehydes are found as primary intermediate products of organic degradation. The production of acetic acid, as a secondary intermediate product, is observed for 2-CEES photooxidation[11] or in a small amount for DES.[10] Both methyl acetate and methyl formate are also formed as secondary intermediates in the former case. Acid products are formed during the photooxidation of 2-CEES on TiO_2-SiO_2 photocatalyst, as indicated by the bands assigned to carboxylate and formate species. This is supported by the fact that the alkyl stretching mode frequencies increase by 2−4 cm^{-1} over the course of the photooxidation reaction. This may be due to the formation of partially oxidized organic species possessing CH_2 and CH_3 groups whose frequency is slightly different from that of 2-CEES. The similarity of behavior for the 2-CEES molecule and the DES molecule upon photooxidation (Figure 4 and Table 1) suggests that Cl substitution in 2-CEES plays little role in governing the overall sequence of reaction events leading to the final oxidation products, CO and CO_2.

Figure 5 shows that different time constants may be associated with the consumption of the alkyl functionalities and the

production of products with single carbonyl groups, with carboxylate groups, and both adsorbed CO and adsorbed CO_2, the final products of oxidation. The "half-life" time constant for the consumption of the alkyl groups is of the order of 40 min, whereas the time constant for the generation of the oxidized species is of the order of 60 min under the conditions of the experiment shown in Figure 5. This difference in time constants implies that multiple photooxidation steps are involved in the conversion of 2-CEES into final oxidation products, but our experiments are not sufficiently sensitive to separate the intermediate surface oxidation steps. Previous study of the photooxidation of 2-CEES on a TiO_2 photocatalyst at 353 K have detected a wide array of intermediate species using GC-MS gas-phase analysis.[11] These experiments, together with our measurements here, suggest that photooxidation causes the cleavage of C−S bonds in 2-CEES. Measurements of the TiO_2-catalyzed photooxidation of DES[10] and dibenzyl sulfide[9] also suggest that C−S bond cleavage generally occurs during photooxidation over TiO_2-based materials.

Acknowledgment. We acknowledge with thanks the support of this work by the DoD Multidisciplinary University Research Initiative (MURI) program administered by the Army Research Office under Grant DAAD19-01-0-0619.

References and Notes

(1) Matthews, R. W. *J. Catal.* **1988**, *113*, 549.
(2) Gao, X.; Wachs, I. E. *Catal. Today* **1999**, *51*, 233.
(3) Anderson, C.; Bard, A. J. *J. Phys. Chem.* **1995**, *99*, 9882.
(4) Anderson, C.; Bard, A. J. *J. Phys. Chem. B* **1997**, *101*, 2611.
(5) Gao, X.; Bare, S. R.; Fierro, J. L. G.; Banares, N. A.; Wachs, I. E. *J. Phys. Chem. B* **1998**, *102*, 5653.
(6) Song, C. F.; Lu, M. K.; Yang, P.; Xu, D.; Yuan, D. R. *Thin Solid Films* **2002**, *413*, 155.
(7) Hoffmann, M. R.; Martin, S. T.; Choi, W.; Bahnemann, D. W. *Chem. Rev.* **1995**, *95*, 69.
(8) Linsebigler, A. L.; Lu, G.; Yates, J. T., Jr. *Chem. Rev.* **1995**, *95*, 735.
(9) Fox, M. A.; Abdel-Wahab, A. A. *Tetrahedron Lett.* **1990**, *31*, 4533.
(10) Vorontsov, A. V.; Savinov, E. V.; Davydov, L.; Smirniotis, P. G. *Appl. Catal. B: Environ.* **2001**, *32*, 11.
(11) Martyanov, I. N.; Klabunde, K. J. *Environ. Sci. Technol.* **2003**, *37*, 3448.
(12) Panayotov, D. A.; Yates, J. T., Jr. *J. Phys. Chem. B*, in press.
(13) Ballinger, T. H.; Wong, J. C. S.; Yates, J. T., Jr. *Langmuir* **1992**, *8*, 1676.
(14) Muha, R. J.; Gates, S. M.; Basu, P. *Rev. Sci. Instrum.* **1985**, *56*, 613.
(15) Basu, P.; Ballinger, T. H.; Yates, J. T., Jr. *Rev. Sci. Instrum.* **1988**, *59*, 1321.
(16) Mawhinney, D. B.; Rossin, J. A.; Gerhart, K.; Yates, J. T., Jr. *Langmuir* **1999**, *15*, 4617.
(17) Rusu, C. N.; Yates, J. T., Jr. *J. Phys. Chem. B* **2000**, *104*, 1729.
(18) Light Sources, Monochromators, Detection Systems; Oriel Corporation, Oriel Catalog; p 82.
(19) Panayotov, D. A.; Yates, J. T., Jr. *Phys. Chem. Lett.*, in press.